



# Numerical simulation of gas and water flow mechanism in hydraulically fractured shale gas reservoirs



Weijun Shen <sup>a, b, c, \*</sup>, Yanmei Xu <sup>d</sup>, Xizhe Li <sup>d</sup>, Weigang Huang <sup>d</sup>, Jiangrui Gu <sup>d</sup>

<sup>a</sup> Key Laboratory for Mechanics in Fluid Solid Coupling Systems, Institute of Mechanics, Chinese Academy of Sciences, Beijing 100190, China

<sup>b</sup> Earth Sciences Division, Lawrence Berkeley National Laboratory, Berkeley, CA 94720, USA

<sup>c</sup> Institute of Porous Flow and Fluid Mechanics, Chinese Academy of Sciences, Langfang, Hebei 065007, China

<sup>d</sup> PetroChina Research Institute of Petroleum Exploration & Development-Langfang Branch, Langfang, Hebei 065007, China

## ARTICLE INFO

### Article history:

Received 23 November 2015

Received in revised form

31 August 2016

Accepted 31 August 2016

Available online 2 September 2016

### Keyword:

Shale gas

Hydraulic fractures

Reservoir properties

Water retention

Gas rate

## ABSTRACT

The problem of the fracturing water remaining in hydraulically fractured shale gas reservoirs has become one of the major concerns in terms of gas productivity and operating costs. The fracturing water retention is influenced by reservoir properties and production parameters, such as matrix porosity and permeability, fracture porosity and permeability, Langmuir pressure and volume, diffusion coefficient, shut-in time, drawdowns and injection rate. In this study, a horizontal well with six-stage hydraulic-fracturing treatment was constructed to understand the water retention and gas production performance in shale gas reservoirs. Gas diffusion, gas adsorption/desorption and Darcy flow as well as non-Darcy flow were considered in this model. The process of water retention and gas production performance was analyzed, and the effects of reservoir and production properties on this problem were performed. The results show that only 34% of the fracturing water can flow back to the surface, most of which remains in shale formations to interfere with gas production. The increasing of matrix porosity, fracture porosity, Langmuir pressure and drawdowns will reduce water retention while water retention in shale matrix will increase with the increasing of matrix permeability and Langmuir volume, and consequently impact gas production. But the trapped water and gas rate increase with the higher fracture permeability. Furthermore, the diffusion coefficient, shut-in time and injection rate do not have a significant effect on water retention and gas productivity. These results can provide insights into a better understanding of gas and water flow in the shale gas reservoirs and the effects of reservoir and production parameters on water retention and gas production.

© 2016 Elsevier B.V. All rights reserved.

## 1. Introduction

Shale gas reservoirs are playing a significant role in satisfying increasing energy demands and having attracted increasing attraction (Shen et al., 2015a). Hydraulic fracturing of horizontal wells is a key technology to produce gas from the ultra-low permeability shale reservoirs. During the hydraulic fracturing process large volumes of the fracturing water are injected into the shale formations to create multiple fractures so that the contact area between fractures and the reservoirs can be largely increased (Cheng, 2012). However, only a small fraction of the fracturing

water, typically 10%–50%, can be recovered back to the surface during the gas production process, most of which remains in the shale matrix due to the high capillary pressure (Engelder et al., 2014; Makhanov et al., 2014). The fracturing water remaining in the shale formations will increase water saturation, and consequently may interfere with gas production (Coskuner, 2006; Cheng, 2012). Thus, understanding the questions such as how much of the fracturing water goes into shale matrix and its effect on gas production are significant for predicting gas shale formation productivity and for optimizing extraction conditions.

Shale is a very fine-grained and clastic sedimentary rock, which has complex pore structures, ultra-low permeability and a variety of storage (Boyer et al., 2006; Strapoc et al., 2010; Shen et al., 2015c). Thus, compared with conventional gas reservoirs, the gas transport in shale gas reservoirs is a complex multi-scale flow process from macro scale to molecular scale (Javadpour et al., 2007). Many

\* Corresponding author. Key Laboratory for Mechanics in Fluid Solid Coupling Systems, Institute of Mechanics, Chinese Academy of Sciences, Beijing 100190, China.

E-mail addresses: [wjshen763@imech.ac.cn](mailto:wjshen763@imech.ac.cn), [wjshen763@gmail.com](mailto:wjshen763@gmail.com) (W. Shen).

research studies on gas flow mechanism of gas shales have been conducted in the recent decade. Ozkan et al., (2009) and Javadpour (2009) proposed that gas flow and diffusion exist at the same time from shale matrix to shale fracture. Dahaghi (2010), Dahaghi and Mohaghegh (2011) successively assumed gas transport in shale would diffuse from shale matrix to shale fracture. Moridis et al., (2010) and Freeman et al., (2011) described and analyzed comprehensively gas flow mechanism in the unconventional shale gas reservoirs, including gas diffusion and desorption from shale matrix to shale fracture, Darcy flow in natural fracture and non-Darcy flow in hydraulic fractures.

Some previous research on fracturing water retention into shale matrix and its impact on gas productivity has been considered in the past. Holditch (1979) supposed that water invasion into matrix is an important cause of low productivity, which reduces the relative permeability to gas and impedes gas production. Solimon and Hunt (1985); Gdanski et al., (2009) presented a numerical simulation to analyze the fracturing fluid cleanup and its effect on gas production. Parekh and Sharma (2004), Mahadevan et al., (2009) and Cheng (2012) successively studied the capillary force effect of water retention in reservoir rocks, and proposed that capillary force had a great effect on water distribution in shale formations. Jurus et al., (2013) used a commercial finite difference model to simulate water injection and observe production performance in horizontal multi-fractured wells. Wang and Leung (2015) modelled the mechanisms of water retention in fracture–matrix system and investigated their associated times scales under different reservoir conditions using the module of CMG-IMEX. However, the impacts of reservoir and production parameters on water retention and gas production have not been systematically studied, and the gas flow transport in gas shales has not been fully considered. Hence, there is a necessity to understand gas and water flow dynamics and the effects of these reservoir and production parameters on the problem so as to optimize gas productivity in shale gas reservoirs.

In this study, we constructed a shale gas reservoir model with six-stage hydraulic fractures using a numerical reservoir simulator of CMG-GEM (CMG GEM User's Guide, 2012). The gas transport processes, including gas diffusion and Langmuir isotherm desorption from shale matrix to shale fracture, Darcy flow in natural fracture and non-Darcy flow in hydraulic fractures, were considered in the model. We first analyze gas and water flow dynamics versus time during the long-term production. Then the effects of the related reservoir properties and production parameters, such as matrix porosity, matrix permeability, fracture porosity, fracture permeability, Langmuir pressure and volume, diffusion coefficient, shut-in time, drawdowns and injection rate, were studied and discussed. The results of these work can provide a better understanding of water and gas flow dynamic and the effects of reservoir and production properties on gas productivity.

## 2. Mathematical model and fluid flow mechanism

### 2.1. Mathematical model

In the stimulation and gas production stages for a hydraulically fractured shale gas well, a two-phase (gas and liquid) flow model or a multi-phase flow model is considered to be sufficient for the modeling work. The fracturing water is usually chosen when stimulating shale gas reservoirs, and consequently the liquid phase flow will occur simultaneously with gas flow during the gas production process. To simplify the problem, it is assumed that there are only gas and water components presented in their associated phases and adsorbed gas within the solid phase of rock. In this study, the dual permeability model is considered to investigate the gas and water flow in hydraulically fractured shale gas reservoirs.

Each fluid phase flows in the matrix and fracture according to the fluid flow mechanism, discussed below. In an isothermal system containing two phases, the fluid flow equation of a dual permeability model (Didier et al., 2014; Shen et al., 2015b) can be described as follow,

$$\frac{\partial}{\partial t} (\varnothing^m S_{\beta}^m \rho_{\beta}^m + v_{sg}) + \nabla \cdot (\rho_{\beta}^m v_{\beta}^m) + q_{\beta}^{mf} + q_{\beta}^m = 0 \quad (1)$$

$$\frac{\partial}{\partial t} (\varnothing^f S_{\beta}^f \rho_{\beta}^f) + \nabla \cdot (\rho_{\beta}^f v_{\beta}^f) - q_{\beta}^{mf} + q_{\beta}^f = 0 \quad (2)$$

where the superscript  $m$  and  $f$  represent the matrix and the fracture, respectively; the subscript  $\beta$  represents the phase ( $\beta = g$  for gas and  $\beta = w$  for water);  $\varnothing$  is the effective porosity;  $S_{\beta}$  is the saturation of the phase  $\beta$ ;  $\rho_{\beta}$  is the density of the phase  $\beta$ ;  $v_{sg}$  is the gas sorption or desorption term;  $v_{\beta}$  is the volumetric velocity vector of the phase  $\beta$ ;  $q_{\beta}^{mf}$  is the exchange term between the matrix and the fracture;  $q_{\beta}$  is the sink or source term of the phase  $\beta$  per unit volume of formation.

### 2.2. Fluid flow mechanism

Compared with conventional gas reservoirs, the pore structure of gas shales is more heterogeneous, including organic matter, nonorganic matrix, natural fractures and pore space induced by hydraulic fractures (Davies et al., 1991; Bustin et al., 2008; Loucks et al., 2009). The giant variation of pores scales makes the flow of gas and water in hydraulically fractured shale gas reservoirs become very complex. The fluid flow in gas shales is controlled by flow mechanism at different scales from the molecular to the macroscopic. In this study, the following mechanism will be considered in the stimulation and production stages and be discussed as follows.

#### 2.2.1. Gas adsorption and desorption

In shale gas reservoirs, the gas adsorbed on organic material surfaces is considered as the main source in the pores (Leathy-Dios et al., 2011). With the pressure decreasing during the gas production, the gas adsorbed on the matrix will release and contribute to the gas production. Thus the gas sorption term is added in Equation (1). For the gas adsorption and desorption in gas shales, several models have been proposed for the reservoirs, but the most commonly used empirical model is the Langmuir isotherm (Langmuir, 1916; Heller and Zoback, 2014). The Langmuir isotherm can be expressed as follows,

$$v_{sg} = v_L \frac{P}{P + P_L} \quad (3)$$

where  $v_{sg}$  is the adsorption mass;  $v_L$  is the Langmuir's volume;  $P$  is the gas reservoir pressure;  $P_L$  is the Langmuir's pressure.

#### 2.2.2. Gas diffusion

Different with conventional gas reservoirs, shale has relatively low porosity and ultra-low permeability, and the pore size is between 1 and 200 nm (Swami et al., 2012). For the nanoscale pores, the gas flow will not follow the Darcy's law, and gas diffusion need to be considered. In the study, the gas diffusion can be expressed as,

$$V = \left( \frac{S}{L_{ij}} \right) \cdot \left( \frac{K_d}{T} \right) \cdot \varnothing_m \cdot S_g \cdot (C(\text{gas}, i) - C(\text{gas}, j)) \quad (4)$$

where  $V$  is the gas phase diffusion rate;  $S$  is the contact area between the block  $i$  and  $j$ ;  $L_{ij}$  is the distance between the block  $i$  and  $j$ ;

$K_d$  is the diffusion coefficient for the hydrocarbon components;  $T$  is the tortuosity of the porous media;  $\phi_m$  is the matrix porosity;  $S_g$  is the smaller of gas saturation in the block  $i$  and  $j$ ;  $C(\text{gas},i)$  and  $C(\text{gas},j)$  are the concentration of the component in the gas phase of the block  $i$  and  $j$ , respectively.

### 2.2.3. Darcy flow

Advection flow is one of the primary driving forces in the porous media, which can be always described by Darcy's law. Shale gas reservoirs contain many nature micro-fractures, and gas molecules flow in the micro-fractures follow Darcy's law. It may be expressed as,

$$v_g = \frac{k_g}{\mu_g} \nabla p \quad (5)$$

where  $v_g$  is the gas flux;  $k_g$  is the gas permeability in the shale rock;  $\mu_g$  is the gas viscosity;  $\nabla p$  is the pressure gradient vector.

### 2.2.4. Non-Darcy flow

Due to the high flow velocity in the hydraulic fractures, the linear Darcy's flow is no longer valid. The gas flow in hydraulic fractures towards the well should be the high velocity non-Darcy flow (Evans and Civan, 1994; Moridis et al., 2010; Freeman et al., 2011). The non-Darcy flow should be described by the Forchheimer modification to Darcy's law given below,

$$-\nabla p = \frac{\mu}{k} v + \beta \rho v^2 \quad (6)$$

where  $\nabla p$  is the pressure gradient vector;  $\mu$  is the viscosity;  $k$  is the permeability;  $v$  is the velocity;  $\rho$  is the phase density;  $\beta$  is the non-Darcy Beta factor.

## 3. Simulation model description

In order to investigate the gas and water flow dynamics in hydraulically fractured shale gas reservoirs, a numerical reservoir simulator of CMG-GEM is used to construct a numerical reservoir model with the dimension of 1100 m  $\times$  900 m  $\times$  60 m, which corresponds to the length, width and height, respectively, as illustrated in Fig. 1. The reservoir has ten shale layers and the total length of horizontal well is 1000 m. The horizontal well is stimulated in the fifth layer with a six-stage hydraulic-fracturing treatment. In each single stage, local grid refinement with logarithmic cell spacing is applied to accurately simulate fluid flow from shale matrix to natural fractures and from natural fractures to hydraulic fractures. Nine transverse fractures are created along the horizontal well with fracture half-length of 130 m, and the spacing of hydraulic fracturing is 100 m. During the fracturing stimulation treatment, the fracturing water is injected into the injector to simulate the hydraulic-fracturing treatment, and the injection rate is 1000 m<sup>3</sup>/d. After two days, the injector is closed while the producer is open to produce for 5000 days with the maximum gas rate of  $1.0 \times 10^5$  m<sup>3</sup>/d. During the gas production, the bottom-hole pressure is controlled by 1.0 MPa.

Table 1 summarizes the detailed reservoir and fracture properties used in the simulation. The reservoir is assumed to be a dual-permeability model, including shale matrix and shale fractures. Due the complex flow in shale gas reservoirs, gas desorption in the matrix, gas diffusion from the matrix to natural fractures, Darcy flow in natural fractures and non-Darcy flow in hydraulic fractures are considered in the simulation. In this study, the water and gas flow in shale matrix and fractures are described with two different sets relative permeability curves based on the previous study

(Deghmoum et al., 2001; Shanley et al., 2004), as shown in Fig. 2. Considering the fracturing water injected during the hydraulic-fracturing treatment, the water-phase imbibition caused by the capillary pressure between water and gas phases is important in the gas production performance. Based on the empirical correlation (Deghmoum et al., 2001; Shanley et al., 2004), the capillary pressure curve used in the matrix is illustrated in Fig. 3. Due to the larger permeability in fractures, the capillary pressure in fractures is considered as zero.

## 4. Results and discussion

### 4.1. Overview

In the beginning, the fracturing water is injected to simulate the hydraulic fracturing treatment, and the injection rate is 1000 m<sup>3</sup>/d for two days. Then the producer is open to produce for 5000 days with the maximum gas rate of  $1.0 \times 10^5$  m<sup>3</sup>/d. As can be illustrated in Fig. 4, the cumulative water is 687 m<sup>3</sup> at the end of 5000 days, which means that 34% of the fracturing water (2000 m<sup>3</sup>) can flow back to the surface during the gas production process. The remaining water (66%) is still retained in shale formations. Some field data has shown that typically 10%–50% of the injected fracturing water could be recovered (King, 2010). From the result of Fig. 4, it is seen that gas rate increases and then decreases, but it is far less than the maximum gas rate. The reason for this phenomenon is that the retained water affects the increasing of gas rate. Fig. 5 shows the variation of water and gas saturation inside matrix at the bottom and top versus time. The water saturation at the bottom and top increases and the gas saturation decreases during the gas production, which indicates the fracturing water flows into shale matrix along the both sides of the horizontal well. Thus it is crucial to deal with the fracturing water after the hydraulic fracturing treatment and thus reduces the retention.

### 4.2. Effect of the matrix porosity

Gas shale is characterized by relatively low porosity, which ranges from 2% to 10% (Boyer et al., 2006). The effects of the matrix porosity between 3% and 9% on water retention and gas production performance have been studied. Fig. 6 shows the variation of water saturation inside matrix (a) and gas rate (b) versus time. It can be seen that the matrix porosity affects directly the fracturing water retention and gas production. With the matrix porosity increasing, water saturation in shale matrix decreases. At the early production time, gas production rate increases linearly, and then increases with matrix porosity increasing. The reason is that water retention in shale matrix decreases with the increase of matrix porosity, and consequently it favors gas flow from shale matrix.

### 4.3. Effect of the matrix permeability

Shale gas reservoir is known for its extra-low permeability which is usually between 0.001 mD to 0.00001 mD (Shen et al., 2015c). This is why it cannot produce economic gas with conventional methods. The matrix permeability values from 0.00001 mD to 0.001 mD are selected to understand water retention and gas production performance. The variation of water saturation inside matrix (a) and gas rate (b) versus time is illustrated in Fig. 7. With the decrease of matrix permeability, the water saturation inside matrix decreases. This is due to the matrix permeability which controls gas flow in shale matrix, and consequently it affects the recovery of fracturing water. As shown in Fig. 7 (b), the lower the matrix permeability is, the higher the gas rate is. This is because water retention in shale matrix makes it difficult to produce gas

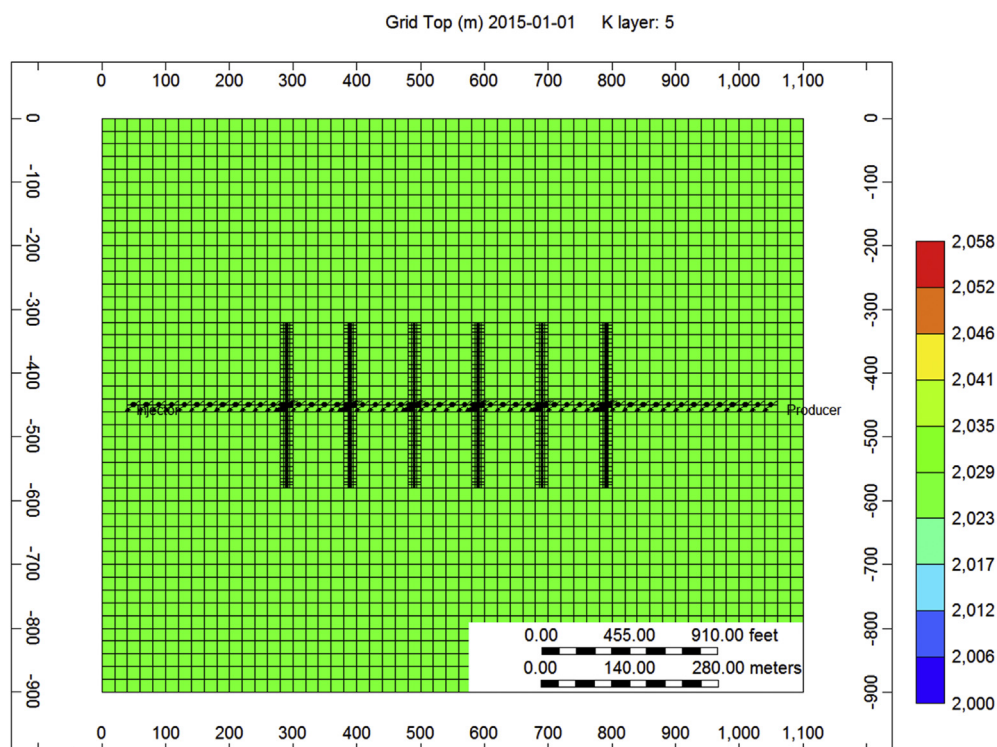


Fig. 1. A numerical reservoir model with six-stage hydraulic fracture treatment.

Table 1

Reservoir and fracture properties used in the simulation.

Parameter	Value	Unit
Model dimension (L × W × H)	1100 × 900 × 60	m
Reservoir depth	2000	m
Initial reservoir pressure	25	MPa
Initial reservoir temperature	70	°C
Rock density	2500	kg/sm <sup>3</sup>
Rock compressibility	$4.0 \times 10^{-6}$	kPa <sup>-1</sup>
Langmuir pressure	1.6	MPa
Langmuir volume	0.09	mol/kg
Initial gas saturation	0.75	value
Gas diffusivity	0.0006	cm <sup>2</sup> /s
Matrix porosity	0.06	value
Matrix permeability	0.0001	mD
Fracture porosity	0.001	value
Fracture permeability	0.01	mD
Bottom-hole pressure	1.0	MPa
Injection rate	1000	m <sup>3</sup> /d
Gas Rate (Max)	$1.0 \times 10^5$	m <sup>3</sup> /d
Horizontal well length	1000	m
Fracture height	60	m
Fracture conductivity	167	mD · m
Fracture half length	130	m
Fracture spacing	100	m
Number of fracture stages	6	value

with the decreasing matrix permeability.

#### 4.4. Effect of the fracture porosity

Shale gas reservoirs are naturally fractured reservoirs, but the narrow fractures are sealed so that gas cannot flow in them (Gale et al., 2007). During the hydraulic fracturing process, the fractures will be activated and reopened, and they will provide the flow pathway for gas (Warpinski et al., 2005). Thus the natural fractures are very significant for gas and water flow in shale formations. The

fracture porosity values between 0.01% and 0.1% are conducted to investigate water retention and gas production performance. Fig. 8 presents the variation of water saturation inside matrix (a) and gas rate (b) versus time. It can be observed that the water saturation inside shale matrix decreases with the increase of fracture porosity. This is because the nature fractures are the main pathway that gas flows from matrix-to-matrix and matrix-to-fracture. From Fig. 8 (b), at the early production time, the gas rate has little change with the fracture porosity decreasing while it increases with the increasing of the fracture porosity later. That means that the increasing fracture porosity favors gas productivity in shale formations.

#### 4.5. Effect of the fracture permeability

Compared with shale matrix, the fractures have relatively higher permeability, which plays an important role in gas and water flow. The effects of the fracture permeability between 0.01 mD and 0.0001 mD are considered in this study. Fig. 9 gives the variation of water saturation inside matrix (a) and gas rate (b) versus time. As illustrated in Fig. 9, with the fracture permeability increasing the water saturation increases rapidly. It suggests the fracturing water flow into shale matrix considerably. The gas rate increases rapidly, and then decreases by a wide margin, especially when the fracture permeability equals to 0.01 mD. The reason is that water retention in shale matrix affects gas flow greatly, and consequently gas rate decreases at the late production time. It is noteworthy that the water retention in shale matrix and gas rate increase with the higher fracture permeability.

#### 4.6. Effect of the Langmuir pressure

Gas desorption is essential to the gas production capacity in shale gas reservoirs (Leathy-Dios et al., 2011). The Langmuir

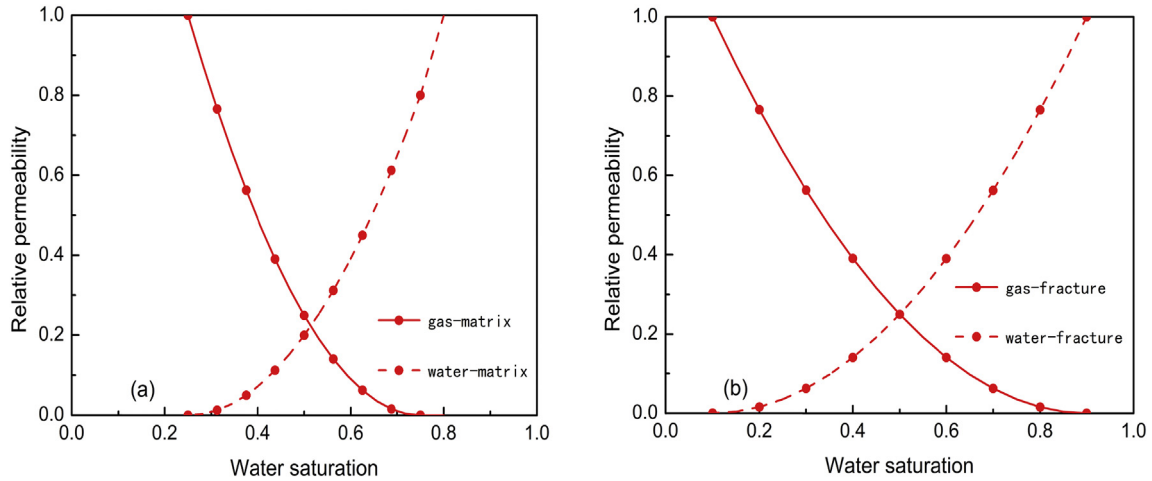


Fig. 2. Two different sets relative permeability curves for shale matrix (a) and shale fracture (b).

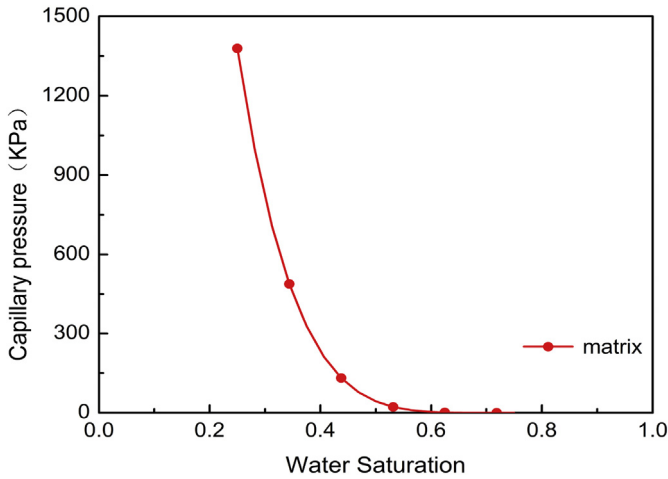


Fig. 3. Capillary pressure curve used in shale matrix.

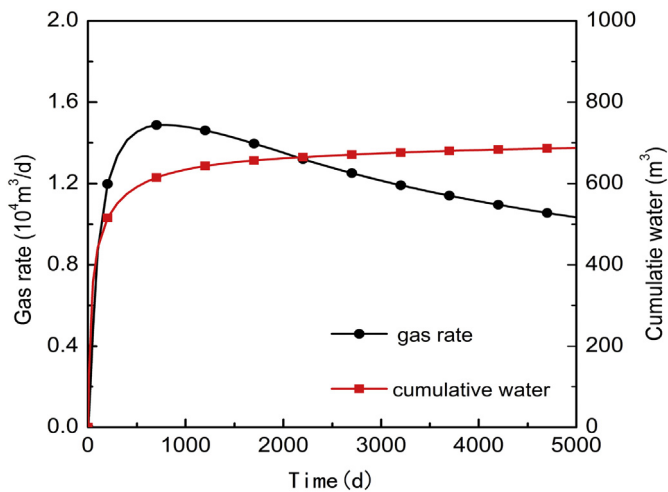


Fig. 4. Variation of gas rate and cumulative water versus time.

pressure is the pressure at which one half of the Langmuir volume can be adsorbed. The Langmuir pressure values from 0.16 MPa to 16 MPa are chosen to study the water retention and gas production performance. The variation of water saturation inside matrix (a)

and gas rate (b) versus time is provided in Fig. 10. At the early gas production, the Langmuir pressure has less effect on water retention. With the increase of the Langmuir pressure, the water retention in shale matrix decreases later. From Fig. 10 (b), it can be seen that as gas production going, the gas rate increases with the Langmuir pressure increasing. This indicates that the Langmuir pressure not only determines gas desorption but also affects gas flow in shale reservoirs. The increasing Langmuir pressure will benefit water recovery and gas production.

4.7. Effect of the Langmuir volume

The Langmuir volume is the maximum amount of gas that can be adsorbed to shale at infinite pressure, which determines gas production performance in shale gas reservoirs. The effects of the Langmuir volume from 0.009 mol/kg to 0.9 mol/kg are selected to study water and gas flow. Fig. 11 shows the variation of water saturation inside matrix (a) and gas rate (b) versus time. It can be observed that water retention into shale matrix decreases with the increase of the Langmuir volume. It implies the increasing Langmuir volume will inhibit water retention. As illustrated in Fig. 11 (b), there is little change on gas rate at the early gas production. However, as gas production going, gas rate will decrease with the decreasing of Langmuir volume. The reason is that gas production in the late is from gas desorption, and the increasing Langmuir volume means that more gas will release from shale matrix and consequently inhibit water retention.

4.8. Effect of the diffusion coefficient

Gas diffusion is one of the main flow mechanisms in the gas production of shale gas reservoirs. The shale matrix contributes to main reservoir storage while the natural fractures provide pathway for gas flow. Gas transport will occur by diffusion from shale matrix to the fractures. The diffusion coefficient values between  $6.0 \times 10^{-3}$  cm/s and  $6.0 \times 10^{-5}$  cm/s are conducted to investigate water and gas dynamics in shale gas formations. The variation of water saturation inside matrix (a) and gas rate (b) versus time is provided in Fig. 12. From Fig. 12 (a), it can be seen that water saturation in shale matrix slightly decreases with the diffusion coefficient increasing. As illustrated in Fig. 12 (b), there is no significant change on gas rate. The result suggested the diffusion coefficient has little effect on water retention and gas production performance.

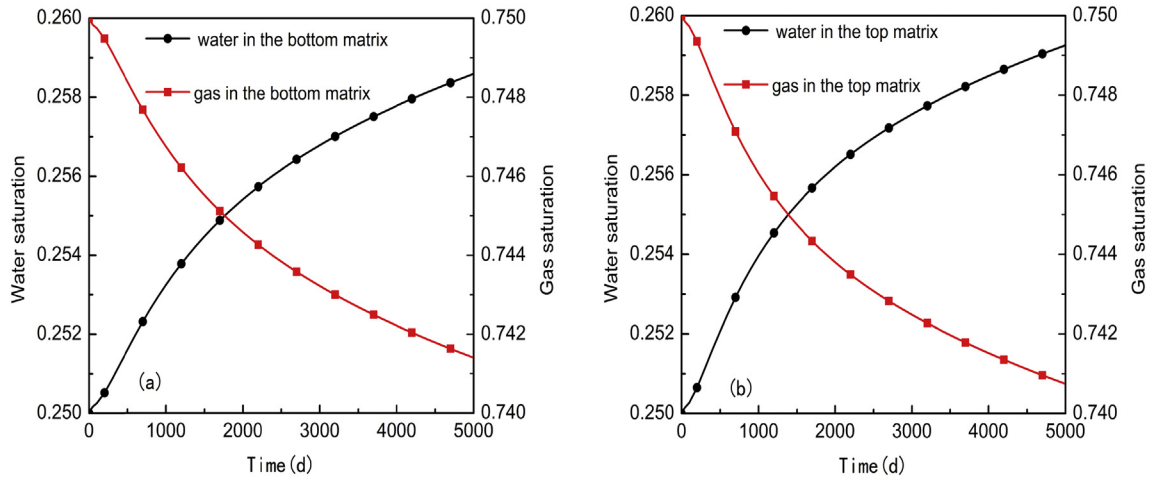


Fig. 5. Variation of water (a) and gas (b) saturation inside matrix versus time.

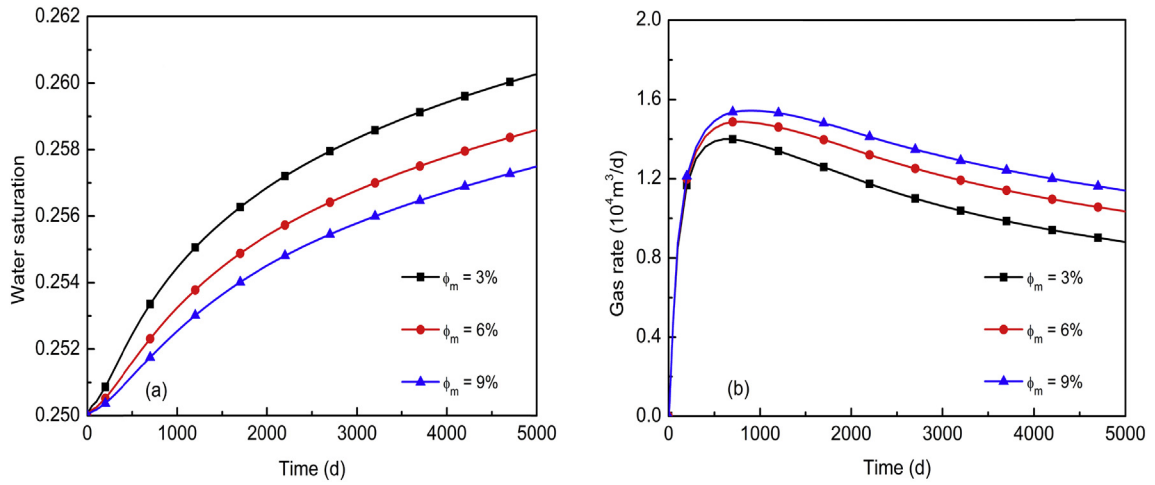


Fig. 6. Variation of water saturation inside matrix (a) and gas rate (b) versus time for matrix porosity.

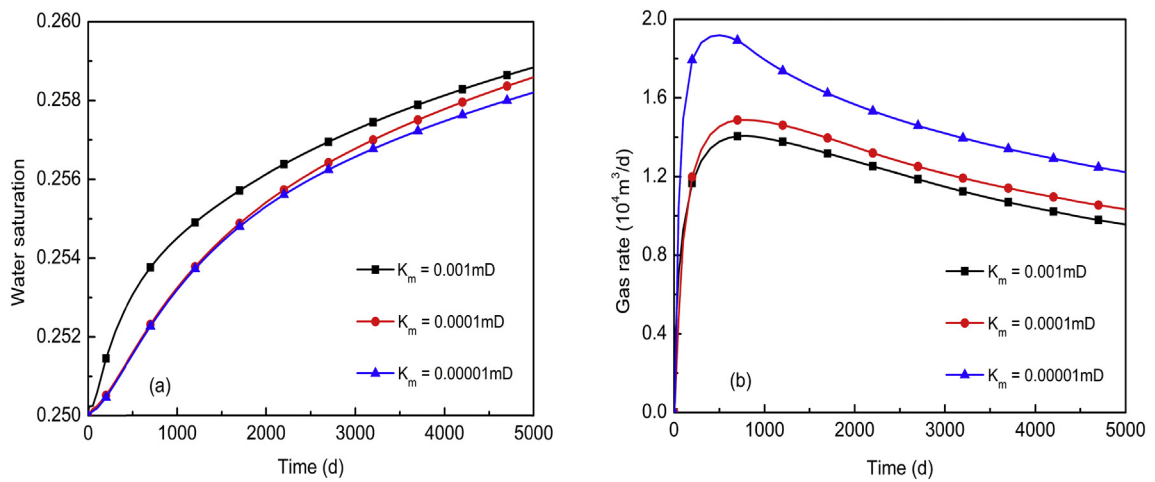


Fig. 7. Variation of water saturation inside matrix (a) and gas rate (b) versus time for matrix permeability.

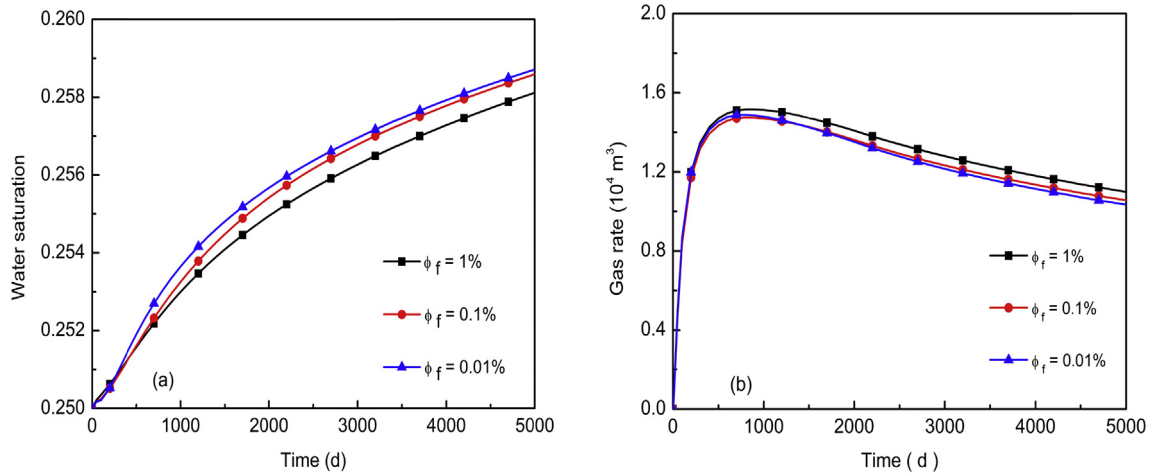


Fig. 8. Variation of water saturation inside matrix (a) and gas rate (b) versus time for fracture porosity.

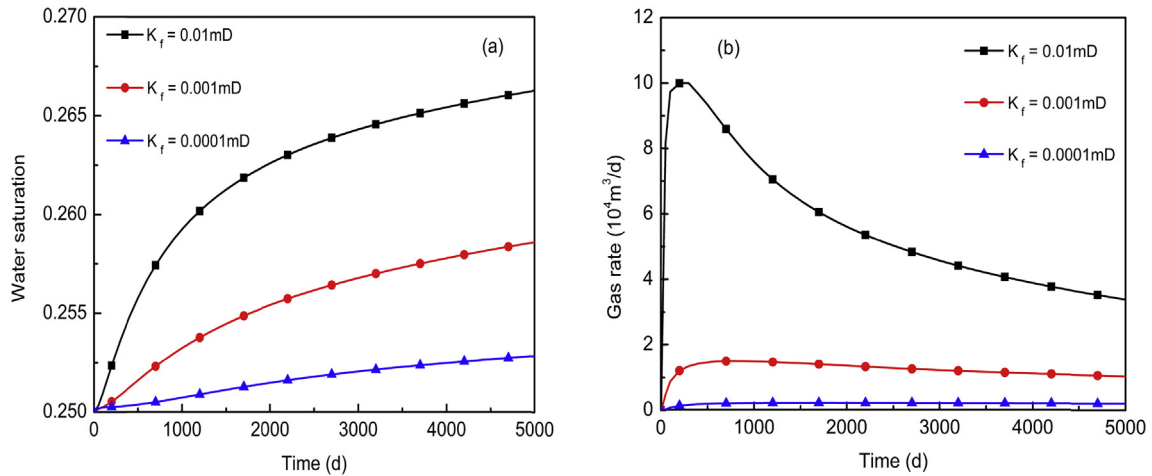


Fig. 9. Variation of water saturation inside matrix (a) and gas rate (b) versus time for fracture permeability.

#### 4.9. Effect of the shut-in time

The shut-in time is an important parameter in the development of shale gas reservoirs, which affects water retention and gas production. The values of the shut-in time from 2 d to 8 d are selected to understand water and gas dynamics in shale gas formations. The variation of water saturation inside matrix (a) and gas rate (b) versus time is provided in Fig. 13. From the result of Fig. 13 (a), we can see that water saturation in shale matrix is almost unchanged with the increasing of shut-in time. Consequently, it doesn't have a significant effect on gas rate, though it rises with the shut-in time increasing in the early stage (Fig. 13 (b)). This implies that the shut-in time has less influence on water and gas dynamics.

#### 4.10. Effect of the drawdowns

The producing drawdowns directly affect gas and water flow in shale gas reservoirs. The values of the different drawdowns between  $1.0 \times 10^3 \text{ kPa}$  and  $4.0 \times 10^3 \text{ kPa}$  are considered in this study. The variation of water saturation inside matrix (a) and gas rate (b) versus time is illustrated in Fig. 14. As shown in Fig. 14 (a), it can be found that with the drawdowns increasing water saturation in shale matrix decreases. While gas rate will rise with the increasing

of the drawdowns from Fig. 14(b). The result indicates that high drawdowns will favor gas production and decrease water retention.

#### 4.11. Effect of the injection rate

To investigate the effects of the injection rate, we change the injection rate from  $1.0 \times 10^3 \text{ m}^3/\text{d}$  to  $2.0 \times 10^3 \text{ m}^3/\text{d}$  to understand water and gas dynamics in shale gas reservoirs. Fig. 15 shows the variation of water saturation inside matrix (a) and gas rate (b) versus time. As illustrated in Fig. 15 (a), it is apparent that water saturation in shale matrix has little change with the injection rate. As a result, it does not affect gas rate in the process of gas production from Fig. 15(b). Thus, the injection rate of the fracturing water does not play an important role in water retention and gas production performance in shale gas reservoirs.

## 5. Conclusions

In this work, considering gas diffusion and Langmuir isotherm desorption from shale matrix to shale fracture, Darcy flow in natural fracture and non-Darcy flow in hydraulic fractures, the gas and water flow dynamics after the hydraulic fracturing treatment were investigated with a numerical model of six-stage hydraulic

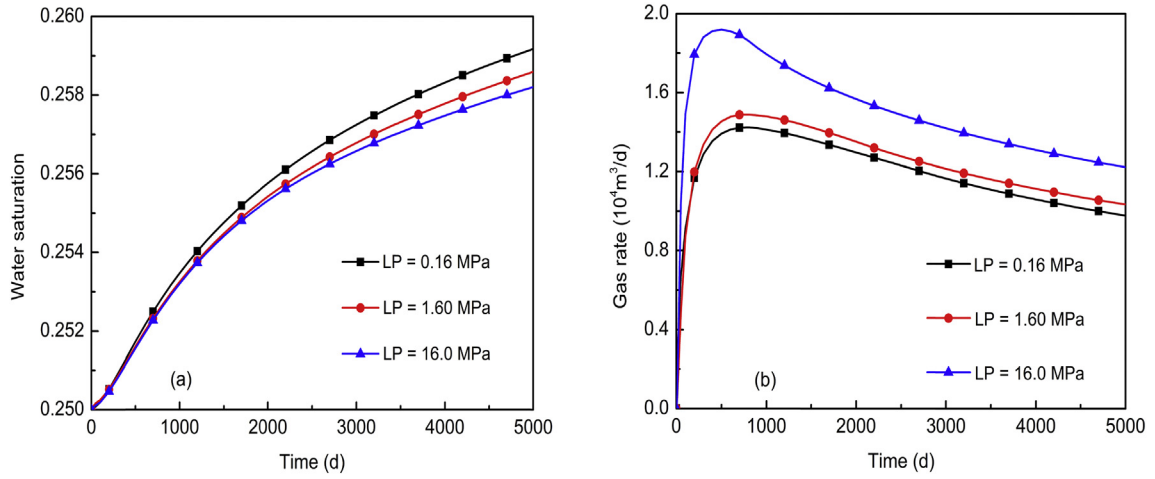


Fig. 10. Variation of water saturation inside matrix (a) and gas rate (b) versus time for Langmuir pressure.

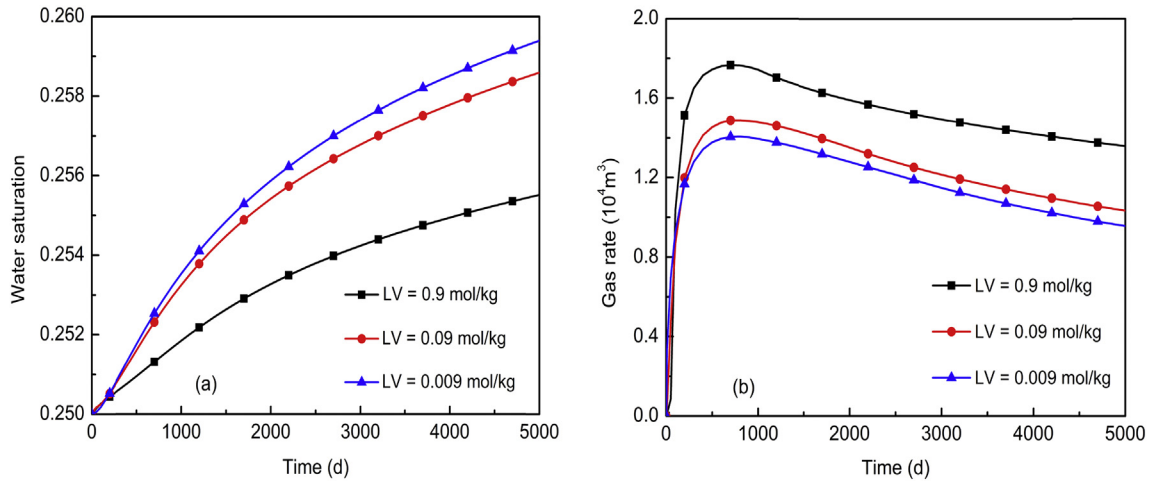


Fig. 11. Variation of water saturation inside matrix (a) and gas rate (b) versus time for Langmuir volume.

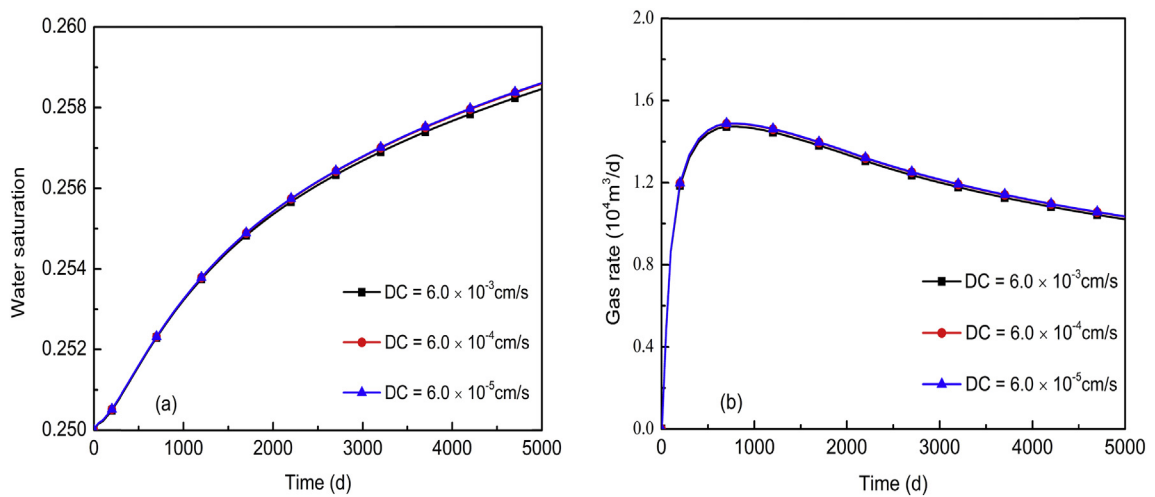


Fig. 12. Variation of water saturation inside matrix (a) and gas rate (b) versus time for diffusion coefficient.



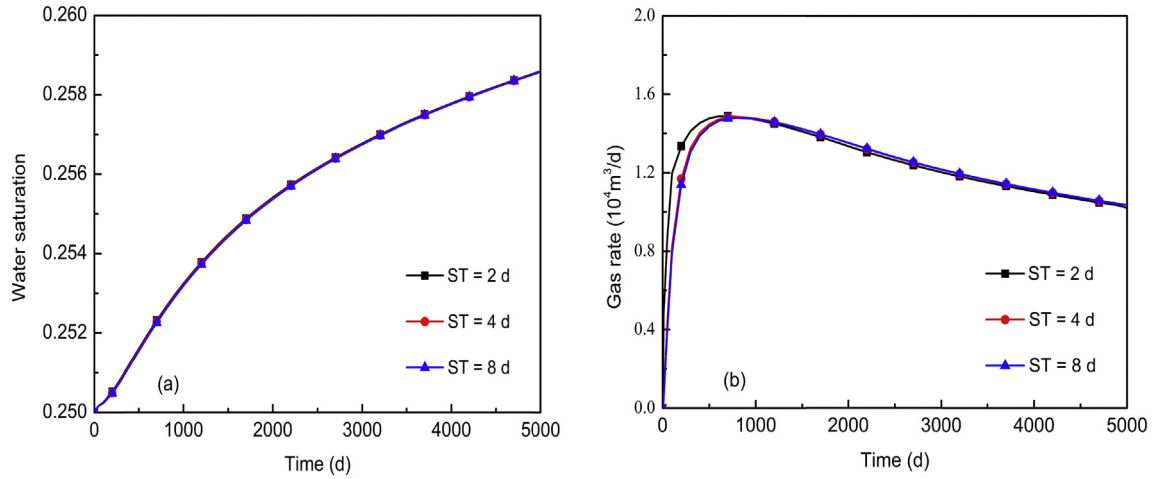


Fig. 13. Variation of water saturation inside matrix (a) and gas rate (b) versus time for shut-in time.

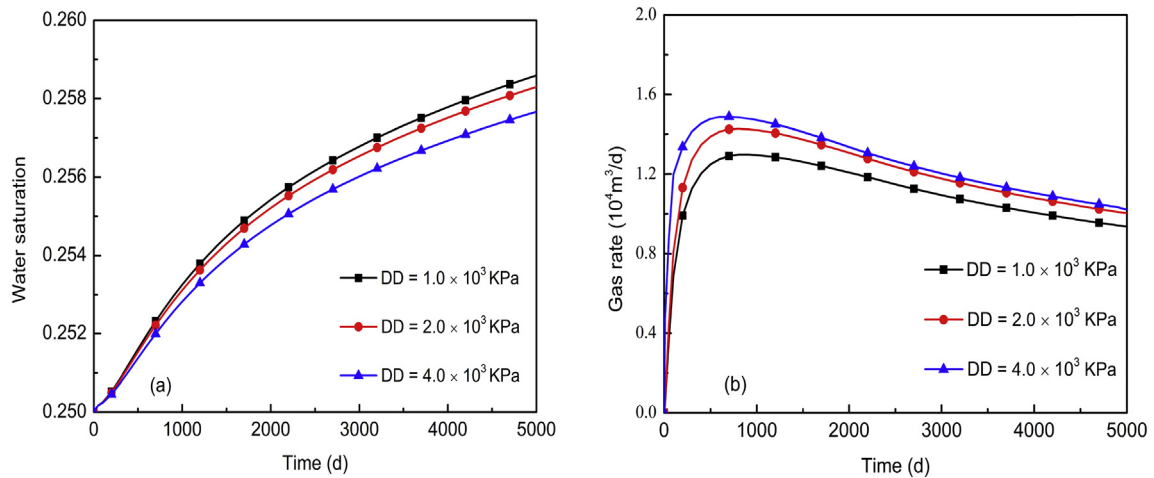


Fig. 14. Variation of water saturation inside matrix (a) and gas rate (b) versus time for different drawdowns.

fractured horizontal well in shale gas reservoirs. The process of water retention and gas production performance was analyzed, and then the effects of reservoir and production properties were

investigated. The following conclusions can be drawn from the simulation study: (1) About 34% of the fracturing water can be recovered in the process of gas production, most of which is

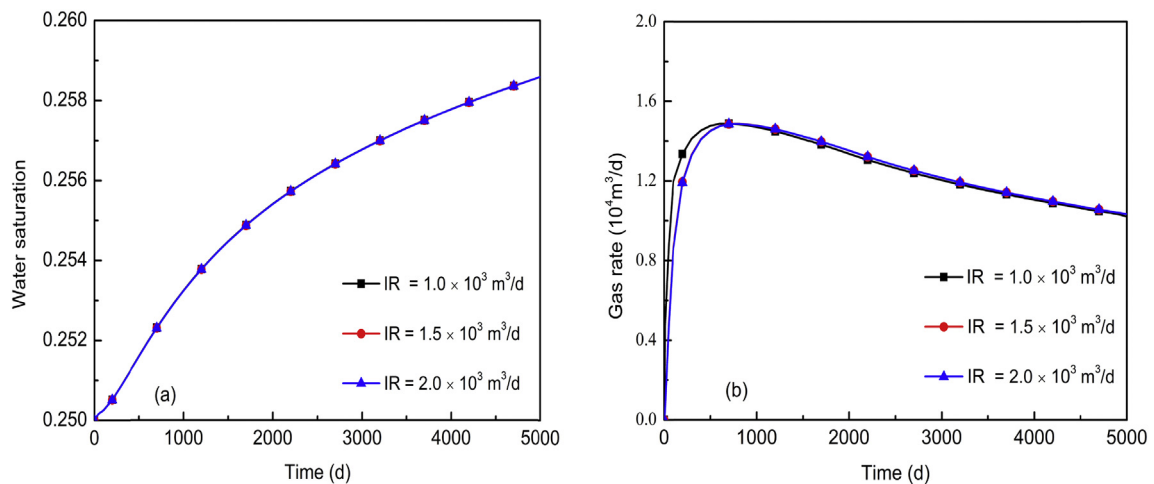


Fig. 15. Variation of water saturation inside matrix (a) and gas rate (b) versus time for injection rates.

trapped in shale formations to interfere with gas production. Consequently it is significant to deal with the fracturing water after the hydraulic fracturing treatment and reduce water retention so as to enhance gas production. (2) With matrix porosity, fracture porosity, Langmuir volume and drawdowns increasing, the fracturing water retention in shale matrix will decrease, and favor gas rate increasing. (3) With the increasing of matrix permeability and Langmuir pressure, the fracturing water remaining in shale matrix will increase, and consequently cause the reduction of gas rate. But the trapped water saturation and the related gas rate will increase with the higher fracture permeability. (4) The changes of diffusion coefficient, shut-in time and injection rate do not have a significant effect on the fracturing water retention and gas production. This work can help to improve the understanding of gas and water flow in the reservoirs and the effects of reservoir and production properties on water retention and gas production.

### Acknowledgments

This work was supported by the National Energy Technology Laboratory under U.S. Department of Energy Contract No. ESD14085, “Understanding Water Controls on Shale Gas Mobilization into Fractures”, and by National Science and Technology Major Project of the Ministry of Science and Technology of China Project (NO. 50150503-12). We also thank the support from the Foundation of China Scholarship Council.

### References

- Boyer, C., Kieschnick, J., Suarez-Rivera, R., et al., 2006. Production gas from its source. *Oilfield Rev.* 18 (3), 36–49.
- Bustin, R.M., Bustin, A.M., Cui, X., et al., 2008. Impact of shale properties on pore structure and storage characteristics. In: *SPE Shale Gas Production Conference*. Fort Worth, Texas.
- Cheng, Y., 2012. Impact of water dynamics in fractures on the performance of hydraulically fractured wells in gas-well reservoirs. *J. Can. Petrol. Technol.* 51 (2), 143–151.
- CMG: GEM User's Guide, 2012. Computer Modeling Group Ltd.
- Coskuner, G., 2006. Completion operation in low permeability deep basin gas reservoirs: to use or not to use aqueous fluids, that is the question. *J. Can. Petrol. Technol.* 45 (10), 23–28.
- Dahaghi, A.K., 2010. Reservoir Modeling of New Albany Shale. West Virginia University, Morgantown, West Virginia.
- Dahaghi, A.K., Mohaghegh, S.D., 2011. A new practical approach in modelling and simulation of shale gas reservoirs: application to New Albany Shale. *Int. J. Oil Gas Coal Technol.* 4 (2), 104–133.
- Davies, D.K., Bryant, W.R., Vessel, R.K., et al., 1991. In: Bennett, R.H., Bryant, W.R., Hulbert, M.H. (Eds.), *Porosity, Permeabilities and Microfabrics of Devonian Shales. Microstructure of Fine-Grained Sediments*. Springer Verlag, New York, pp. 109–119.
- Deghmoum, A.h., Tiab, D., Mazouzi, A., 2001. Relative permeability in dual porosity porous media. *J. Can. Pet. Technol.* 40 (12), 32–42.
- Didier, Y.D., Wu, Y.S., Farah, N., et al., 2014. Numerical simulation of low permeability unconventional gas reservoirs. In: *SPE SPE/EAGE European Unconventional Conference and Exhibition*. Vienna, Austria.
- Engelder, Cathles, L.M., Bryndzia, L.T., 2014. The fate of residual treatment water in gas shale. *J. Unconv. Oil Gas. Resour.* 1, 33–48.
- Evans, R.D., Civan, F., 1994. Characterization of non-Darcy multiphase flow in petroleum bearing formations. In: Report, US DOE Contract No. DE-AC22-90BC14659. School of Petroleum and Geological Engineering, University of Oklahoma.
- Freeman, C.M., Moridis, G.J., Blasingame, T.A., 2011. A numerical study of microscale flow behavior in tight gas and shale gas reservoir systems. *Transp. Porous Med.* 90, 253–268.
- Gale, J.F.W., Reed, R.M., Holder, J., 2007. Natural fractures in the Barnett Shale and their importance for hydraulic fracture treatments. *AAPG Bull.* 91 (4), 603–622.
- Gdanski, R., Fulton, D., Shen, C., 2009. Fracture-face skin evolution during cleanup. *SPE Prod Opera* 24 (1), 22–34.
- Heller, R., Zoback, M., 2014. Adsorption of methane and carbon dioxide on gas shale and pure mineral samples. *J. Unconv. Oil Gas. Resour.* 2014 (8), 14–24.
- Holditch, S.A., 1979. Factors affecting water blocking and gas flow from hydraulically fractured gas wells. *J. Petrol. Technol.* 31 (12), 1515–1524.
- Javadpour, F., 2009. Nanopores and apparent permeability of gas flow in mudrocks (shales and siltstone). *J. Can. Pet. Technol.* 48 (8), 16–21.
- Javadpour, F., Fisher, D., Unsworth, M., 2007. Nanoscale gas flow in shale gas sediments. *J. Can. Pet. Technol.* 46 (10), 16–21.
- Jurus, W.J., Whitson, C.H., Golan, M., 2013. Modeling water flow in hydraulically fractured shale wells. In: *SPE Annual Technical Conference and Exhibition*. New Orleans, Louisiana.
- King, G.E., 2010. Thirty years of shale fracturing: what have we learned. In: *SPE Annual Technical Conference and Exhibition*. Florence, Italy.
- Langmuir, I., 1916. The constitution and fundamental properties of solids and liquids. *J. Am. Chem. Soc.* 38 (11), 2221–2295.
- Leathy-Dios, A., Das, M., Agarwal, A., et al., 2011. Modeling of transport phenomena and multicomponent sorption for shale gas and coalbed methane in an unstructured grid simulator. In: *SPE Annual Technical Conference and Exhibition*. Denver, Colorado.
- Loucks, R.G., Reed, R.M., Jarvie, D.M., et al., 2009. Morphology, genesis and distribution of nano-scale pores in siliceous mudstones of the mississippian Barnett Shale. *J. Sed. Res.* 79 (12), 848–861.
- Mahadevan, J., Le, D., Hoang, H., 2009. Impact of capillary suction on fracture face skin evolution in waterblocked wells. In: *SPE Hydraulic Fracturing Technology Conference*. Woodlands, Texas.
- Makhanov, K., Habibi, A., Dehghanpour, H., et al., 2014. Liquid uptake of gas shales: a workflow to estimate water loss during shut-in periods after fracturing operations. *J. Unconv. Oil Gas. Resour.* 7, 22–32.
- Moridis, G.J., Blasingame, T.A., Freeman, C.M., 2010. Analysis of mechanisms of flow in fractured tight gas and shale gas reservoirs. In: *SPE Latin American and Caribbean Petroleum Engineering Conference*. Lima, Peru.
- Ozkan, E., Brown, M., Raghavan, R.S., et al., 2009. Comparison of fractured horizontal-well performance in conventional and unconventional reservoirs. *SPE Res. Eva. Eng.* 14 (2), 248–259.
- Parekh, B., Sharma, M.M., 2004. Cleanup of water blocks in depleted low-permeability reservoirs. In: *SPE Annual Technical Conference and Exhibition*. Houston, Texas.
- Shanley, K.W., Cluff, R.M., Robinson, J.W., 2004. Factors controlling prolific gas production from low-permeability sandstone reservoirs: implications for resource assessment, prospect development, and risk analysis. *AAPG Bull.* 88 (8), 1083–1122.
- Shen, W.J., Zheng, L.G., Oldenburg, C.M., et al., 2015a. Methane diffusion and adsorption in shale rocks—A numerical study using the dusty gas model in Tough2/EOS7C-ECBM. In: *TOUGH Symposium*. Lawrence Berkeley National Laboratory, Berkeley, California.
- Shen, W.J., Liu, X.H., Li, X.Z., et al., 2015b. Water coning mechanism in Tarim fractured sandstone gas reservoirs. *J. Cent. South Univ.* 22, 344–349.
- Shen, W.J., Wan, J.M., Kim, Y., et al., 2015c. Porosity calculation, pore size distribution and mineral analysis within shale rocks: application of scanning electron microscopy. *Elec. J. Geotech. Eng.* 20, 11477–11490.
- Solimon, M.Y., Hunt, J.L., 1985. Effect of fracturing fluid and its cleanup on well performance. In: *SPE Eastern Regional Meeting*. Morgantown, West Virginia.
- Strapoc, D., Mastalerz, M., Schimmelmann, A., et al., 2010. Geochemical constrains on the origin and volume of gas in the New Albany Shale (Devonian-Mississippian), eastern Illinois Basin. *AAPG Bull.* 94, 1713–1740.
- Swami, V., Clarkson, C.R., Settari, A., 2012. Non-Darcy flow in shale nanopores: do we have a final answer. In: *SPE Canadian Unconventional Resources Conference*. Calgary, Alberta.
- Wang, M.Y., Leung, J.Y., 2015. Numerical investigation of fluid-loss mechanisms during hydraulic fracturing flow-back operations in tight reservoirs. *J. Pet. Sci. Eng.* 133 (2015), 85–102.
- Warpinski, N.R., Kramm, R.C., Heinze, J.R., et al., 2005. Comparison of single- and dual-array microseismic mapping techniques in the Barnett Shale. In: *SPE Annual Technical Exhibition*. Dallas, Texas.